A major purpose of the Technical Information Center is to provide the broadest dissemination possible of information contained in DOE's Research and Development Reports to business, industry, the academic community, and federal, state and local governments.

Although a small portion of this report is not reproducible, it is being made available to expedite the availability of information on the research discussed herein.

1

LA-UR –00-200U

CCT 0 G 1968

TITLE: **HIGH TEMPERATURE INTERDIFFUSION AND PHASE EQUILIBRIA IN U-Mo**

LA-UR--88-2660

DE89 000395

AUTHOR(S): Lynn B. Lundberg

MASTER

Los Alamos Los Alamos National Laboratory
Los Alamos, New Mexico 87545

FORM NO 836 R4
ST NO 2629 5/81

HIGH TEMPERATURE INTERDIFFUSION
AND PHASE EQUILIBRIA IN U-Mo

by

Lynn B. Lundberg

Abstract

Experimental data for interdiffusion and phase equilibria in the U-Mo system have been obtained over the temperature range 1400 to 1525 K as a fallout from compatibility experiments in which UO_2 was decomposed by lithium in closed molybdenum capsules. Composition-position, x-ray diffraction and microstructural data from the interdiffusion zones indicate that the intermediate phase U_2Mo is found in this temperature range, contrary to the currently accepted equilibrium U-Mo phase diagram. The U-Mo interdiffusion data are in good agreement with published values. Inclusion of the U_2Mo phase in a theoretical correlation of interdiffusion and phase equilibria data using Darken's equation indicate that high temperature interdiffusion of uranium and molybdenum follows the usual thermodynamic rules. Significant changes in the value of the thermodynamic based Darken factor near the U_2Mo phase boundary on the high uranium side are indicated from both the new and published interdiffusion data.

I. Introduction

During a recent experimental verification of the incompatibility of uranium dioxide with pure lithium at high temperatures, uranium metal was produced and interdiffused with the molybdenum capsule that had contained the reactants. U-Mo interdiffusion data were obtained over the temperature range 1400 to 1525 K. The microstructures and micro-chemical analyses of the resultant interdiffusion zones were only partly consistent with the most recent published equilbrium U-Mo phase diagram[1]. Because of the significance of this alloy system in nuclear technology, these results were examined in light of the thermodynamic aspects of the interdiffusion as it relates to the high temperature phase equilibria of the U-Mo system.

Because local thermodynamic is maintained in a diffusion couple, the interdiffusion of two pure elements at constant temperature can produce only those binary phases that can exist in thermodynamic equilibrium in the alloy system. This direct correlation between phase equilbria and isothermal interdiffusion makes it possible to determine the alloy phase diagrams directly from micro-chemical analysis of the phases observed in interdiffused samples.

Data on the interdiffusion of uranium and molybdenum and tracer diffusion of both elements in U-Mo alloys have been reviewed by Fedorov and Smirnov [2]. These authors concluded that U-Mo interdiffusion in γ-uranium, the body-centered-cubic allotrope of uranium, was anomolous as they were unable to calculate interdiffusion coefficients from Darken's equation [3] that

compared with published values [4]. For these calculations, Fedorov and Smirnov [2] had used tracer diffusion coefficients for both uranium and molybdenum that they had obtained for U-Mo alloys containing 0 to 30 at.% Mo along with published thermodynamic data [5]·

The most recent, complete binary phase diagram for U-Mo [1] indicates that in the temperature range 1400 to 1525 K molybdenum can contain up to about 2.5 at.% uranium in solid solution.

The published phase diagram also indicates that γ-uranium can dissolve up to about 43 at.% molybdenum in this temperature range. No intermediate phases are reported in this temperature range even though the intermetallic compound U_2Mo is reported for temperatures below 875 K.

II. Experimental

A. Materials and Procedures

In the compatibility experiments, UO_2 shards, broken from a cold-pressed and sintered disc, were immersed in lithium and sealed inside a capsule made from commercial, pure molybdenum. Each of the four capsules from which data relevant to this study was obtained contained 1 g of UO_2 and approximately 20 cm^3 of pure lithium.

The UO_2 was determined to be very close to the stoichiometric composition, and its overall purity was quite high as it contained less than 10 wppm of any impurity element that could be detected by mass spectrographic methods. The uranium in the UO_2 consisted of 6% ^{235}U and the remainder ^{238}U. The lithium stock used to fill the capsules was chemically analyzed and found to contain 0.068 at.% O, 0.0042 at.% C, 0.0014 at.% N and 0.0003 at.% U.

The capsules were fabricated from seamless molybdenum tubing which had an outside diameter of 25.4 mm and of wall thickness 1.78 mm. End caps for the capsules were machined from bar stock. Both the tubing and the end-caps were produced from low carbon arc-cast molybdenum stock. These end-caps were electron beam welded into one end of each tube prior to loading with UO_2 and lithium. The finished capsules had an interior length of 69 mm. All capsule parts were vacuum annealed for 1h at 1700 K as a final cleaning step just prior to loading. Chemical analysis of the tubing and bar stock indicated both contained less than 0.02 at.% each of C, O, N, Si, and Fe as the major impurities.

All capsules were loaded with UO_2 and lithium inside a high-purity argon glove-box. The purity of the argon in the glove-box was maintained by continuous circulation through a commercially available purification train that was capable of removing water, oxygen, nitrogen and other reactive gases to measured volumetric concentrations of 15 ppm or less. The UO_2 shards, previously weighed on a microbalance located in the glove box, were placed in the capsule and covered with molten lithium that was forced from an external reservoir by ultra-high purity argon

gas pressure.

It was necessary to keep the lithium out of the end cap joint region so that it would not interfere with the final weld closure process. The closure end-cap was pressed into each capsule after loading, and each partially sealed capsule was placed inside a sealed bottle for removal from the glove-box and transport to the electron beam welding facility. When ready for final closure, each capsule was taken from its transport bottle in ambient air and immediately placed in the welding chamber. After immediate evacuation of the welding chamber, each capsule was held in the dynamically pumped vacuum chamber for several hours prior to welding. Each capsule probably contained a small pressure of high-purity argon after the seal weld was performed because each end cap fit rather snugly into its respective capsule inhibiting the capsule evacuation process. Air contamination of the contents of these capsules was never indicated visually or by chemical analysis.

The sealed capsules were heated in an electric, radiant-heated, cold-wall vacuum furnace equipped with resistance heating elements made of tungsten mesh and heat shields made of tungsten foil. One capsule was heated 498 h at 1400 K, another was heated 10 h at 1450 K. Two other capsules were heated 10 h at 1525 K. The shorter anneals were continuous, while the longest heat treatment was interrupted several times for nondestructive, x-radiographic examinations of the capsule. Temperatures were measured with a W-5Re/W-25Re thermocouple whose bare junction was located near the center of the hot zone of the furnace, close to the capsule. The furnace temperature was controlled within ±1° of the desired value. The expected accuracy of this type of thermocouple is about ±10° in the temperature range of the anneals. The furnace chamber vacuum was maintained at less than 7×10^{-5} Pa during all heat treatments. Due to the fact that the furnace was a cold wall design, cooling of the sample at the end of the heat treatment was rapid. Cooling rates from the heat treatment temperatures to below 1000 K were of the order of 1°/s.

Each heat-treated capsule was opened inside the high-purity argon glove-box. Solid lithium core samples were removed from each capsule, immediately weighed in the glove-box, and transported inside bottles, tightly sealed before removal from the glove-box, to the analysts for determination of oxygen, nitrogen, carbon, uranium and molybdenum. One sample from each capsule was used for the oxygen determination using a fast-neutron activation method. Because the oxygen determination was nondestructive, this same sample was also used for both uranium and molybdenum determinations using x-ray fluorescence methods. A second lithium sample was taken from each capsule for carbon analysis using microcombustion methods, and a third sample was taken for nitrogen analysis using the Kjeldahl method.

The lithium remaining in each capsule was melted and shaken out as much as possible in the glove-box. Residual lithium was removed from each capsule by reaction with water.

The bottom and side of each capsule were sectioned through and prepared for metallographic and microprobe examinations. Electron and ion microprobe analyses were performed on the flat, polished surfaces. Minimum detection limits for the electron microprobe for both molybdenum and uranium were of the order of 0.5 at.%. The ion microprobe was used for qualitative analysis of the

light elements that could not be detected by the electron microprobe.

The electron microprobe used in this study was a Cameca Model MBX capable of detecting elements with atomic numbers as low as 12. This electron microprobe was equipped with three wavelength dispersive spectrometers, one energy dispersive spectrometer, and both secondary and backscattered electron detectors. The electron microprobe analysis system included both automatic data collection equipment and an integrated microcomputer for data reduction. The ZAF microcomputer routine was used for the conversion of the x-ray intensities to element content.

Metallographic samples that were exposed to air for extended periods of time were found to be covered with an oxide over major areas of the U-Mo alloys that had to be removed before accurate electron microprobe analyses could be performed. These oxide layers were removed by either ion milling or mechanical polishing of the surfaces immediately before placing each sample into the vacuum chamber of the electron microprobe. After proper cleaning of the surfaces, oxygen was no longer detected and accurate molybdenum and uranium content data were obtained. Concentration-position data were obtained for samples taken from the capsules anealed at 1400 and 1525 K.

The capsule that was heated at 1400 K had a sufficient amount of single phase U-Mo alloy product formed on the bottom to collect a sample for x-ray diffraction analysis. A Debye-Sherrer powder x-ray diffraction sample was obtained by mechanically removing this material from the bottom of the capsule under a pure argon atmosphere. Some of the powdered sample material was sealed in an evacuated quartz capillary for irradiation in the powder camera. One x-ray diffraction pattern was obtained from the encapsulated sample at room temperature using Mo-Kα radiation. The film record was analyzed producing a set of d-spacings and relative diffraction line intensities.

3. Results

All heat treatment conditions caused complete reduction of the UO_2 by the lithium, and the product uranium diffused into the molybdenum capsules. The chemical analysis of the lithium samples removed from the capsules indicated that the oxygen, carbon, and nitrogen levels were only slightly higher than the original values. If all of the oxygen from the reduction of the UO_2 had dissolved in the lithium in each capsule, the final oxygen concentration in the lithium would have been 0.5 at.% in all cases. However, the highest oxygen level found in the post-heat treatment lithium was 0.15 at.%. Carbon content of the lithium taken from the heat-treated capsules never exceeded 0.03 at.%, while the nitrogen content was measured at 2.3 at.% in the 1450 K capsule but less than 0.01 at.% in the others. Uranium concentration in the exposed lithium was below 0.00015 at.%.

Although most of the product uranium metal remained at the bottom of each capsule and alloyed with its bottom end-cap, uranium was found to have also been distributed over all of the interior surfaces of each capsule. In no instance was a capsule breached due either to reaction with

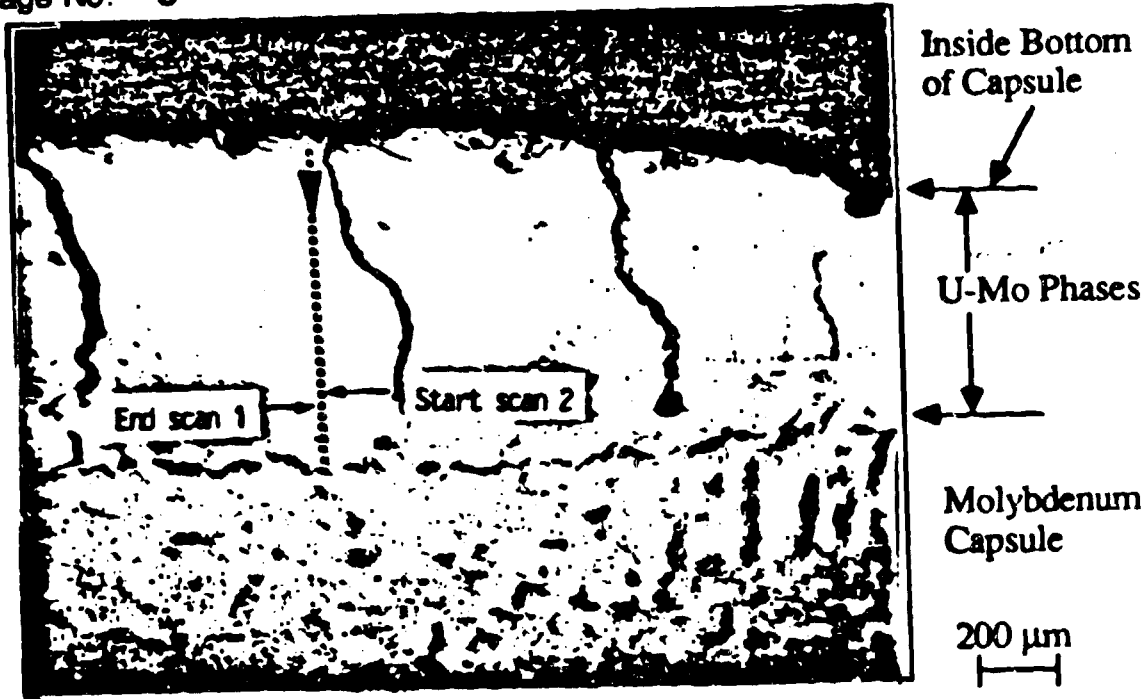uranium or any other consequence of the heat treatment.

1. 1400 K Capsule Data

Two views of typical microstructures of the cross-section of the bottom of the molybdenum capsule that contained lithium and UO_2 at 1400 K for 498 h are presented in Fig. 1. X-radiographs of the unopened capsule looking through the bottom had indicated that most of the uranium had remained very close to the original location of the UO_2 shards. The microstructures seen in Fig. 1 result from interdiffusion of uranium with the capsule bottom. As can be seen in Fig. 1(a), the diffusion zone formed on the bottom of the molybdenum container is separated into three distinct layers. Neither oxide nor carbide particles were observed in the microstructure of the phases indicated by these layers, and neither oxygen nor carbon were detected in this sample with either the electron or ion microprobe scans of these areas.

The microstructural feature marked A in Fig. 1(b) appears to have been molten at the test temperature of 1400 K. This feature was analyzed by the electron microprobe and found to contain only uranium. The holes seen associated with these uranium globules appear to be Kirkendall voids which resulted from the rapid diffusion of uranium into the surrounding solid alloy.

The composition-position data from the two electron microprobe scans marked in Fig. 1(a) are plotted together in Fig. 2. This plot clearly indicates the large compositional discontinuity between the thickest layer seen in in Fig. 1(a) and the phase layer next to the unreacted region of the molybdenum capsule.

The molybdenum-rich U-Mo alloy phase, seen in Fig. 1(a) as a band adjacent to the pure molybdenum of the capsule bottom, was analyzed with the electron microprobe and found to contain up to 1.1 at.% U. A similar uranium bearing layer was also observed over most of the inside surface of the capsule. The most abundant phase seen in both views in Fig. 1 was measured and found to contain from 63.6 to 69.2 at.% U. Molybdenum was the only other element detected in this layer by the electron microprobe. This phase will be designated U_2Mo in the following discussions because of its composition and physical characteristics. The spot marked B in Fig. 1(b) was analyzed to be U-35 at.% Mo. The cracks through the U_2Mo layer seen in Fig. 1(a) suggest that this phase is brittle and has higher thermal expansion than molybdenum.

Inside Bottom
of Capsule

U-Mo Phases

Molybdenum
Capsule

200 μm

End scan 1   Start scan 2

(a)

Inside Bottom
of Capsule

40 μm

(b)

Fig. 1. Cross-sectional views at two magnifications of the bottom of the molybdenum capsule that contained lithium and UO_2 for 498 h at 1400 K.
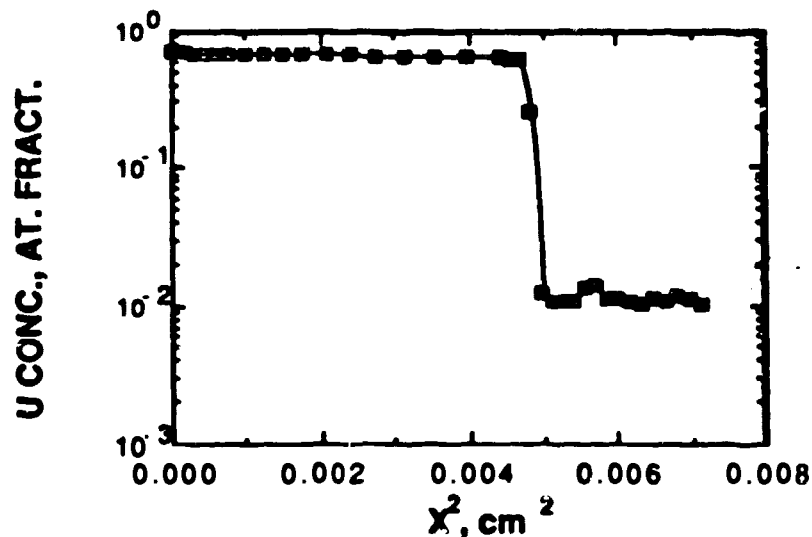
Fig. 2. Uranium concentration profile through reaction layer at the bottom of molybdenum capsule that contained lithium and UO_2 for 498 h at 1400 K.

The concentration-position data for the U_2Mo region of scan 1 in Fig. 1(a) has been plotted in terms of the natural logarithm of the uranium concentration and the square of the position coordinate in Fig. 3. The linear character of this curve suggests that the diffusion process may be treated as one-dimensional interdiffusion between a finite-quantity component, U, and an infinite-quantity component, Mo. According to the solution of Fick's second law for these boundary conditions, the slope of ln, curve in Fig. 3 is equal to $1/4Dt$, where t is the interdiffusion time at constant temperature. The best linear-fit for these data gives $D_{U-Mo} = 6.6 \times 10^{-9}$ cm^2/s.

The thickness of the inner layer seen in Fig. 1(a) averaged 160 µm. The one-dimensional parabolic rate constant for the growth of this layer is 3.6×10^{-11} cm^2/s. This layer appears to have been formed by the interdiffusion of molybdenum and U_2Mo which means that its parabolic growth rate constant can be interpreted as an interdiffusion coefficient for these two solid phases.

The x-ray diffraction pattern obtained from material broken from the bottom of this capsule

indicated that only molybdenum and an unidentfied phase were present. Neither γ-uranium nor uranium oxide diffraction lines could be identified in this pattern. The d-spacings and relative intensities for those diffraction lines associated with the unknown phase are listed in Table 1. This pattern was indexed to a close-packed hexagonal lattice with lattice constants $a=0.330$ nm and $c=0.475$ nm. The planar indices for this lattice are also listed in Table I.
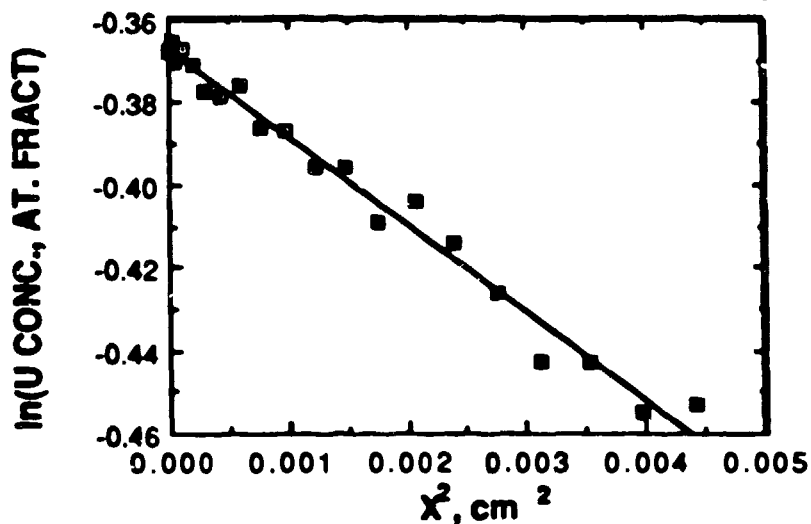
Fig. 3.   Uranium concentration profile through U_2Mo in bottom of Mo capsule heated for

498 h at 1400 K with lithium and UO_2 inside.

Table I.   X-ray diffraction powder pattern less Mo-lines for U-Mo residue in the bottom of the

molybdenum capsule that contained UO_2 and Li at 1400 K for 498 h.

d-spacing (nm)	I/I_0	hkl (hcp lattice)
0.285	20	100
0.245	10	101
0.2375	100	002
0.183	10	102
0.165	10	110
0.142	10	200
0.139	10	103
0.138	10	201
0.137	10	112

2. 1450 K Capsule Data

Microstructures of the product phases formed at the bottom of the capsule that was heated at

1450 K for 10 hours with UO_2 and lithium inside are seen in Fig. 4. Four different structures can

be seen in this photomicrograph. These microstructures include the capsule molybdenum, a band

of uranium dissolved in molybdenum. Mo[U] (near C in Fig. 4(a)). a band of U_2Mo (B in both

4(a) and 4(b)), and a band of a mixture of uranium and U_2Mo.

The electron microprobe data indicated that the single-phase appearing material designated B

in Fig. 4(a) contained 30 at.% Mo and 70 at.% U near the inner surface of the capsule and 38 at.% Mo and 62 at.% U near the Mo[U] band near C. The electron microprobe data indicated that the Mo[U] band contained 98-99 at.% Mo and 1-2 at.% U. The Mo[U] layer measures about 50 μm thick which translates to an interdiffusion coefficient of 2×10^{-10} cm²/s.
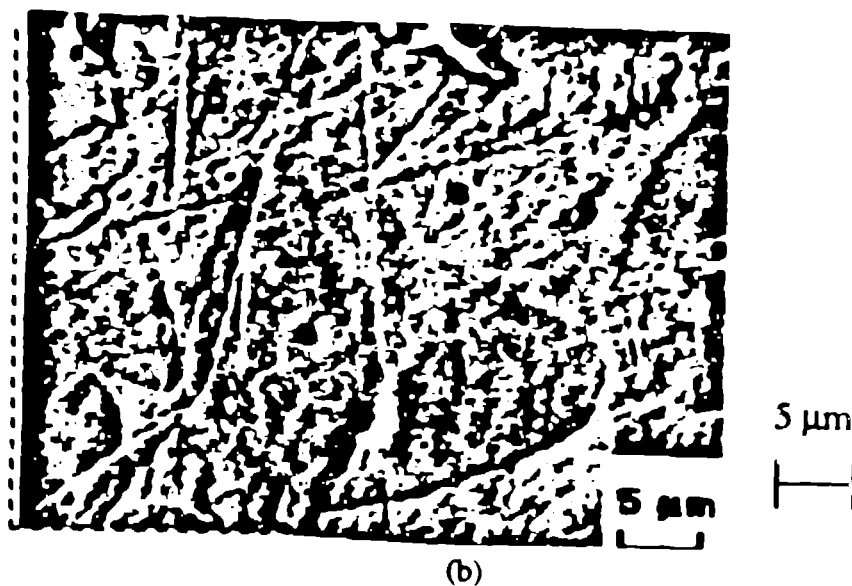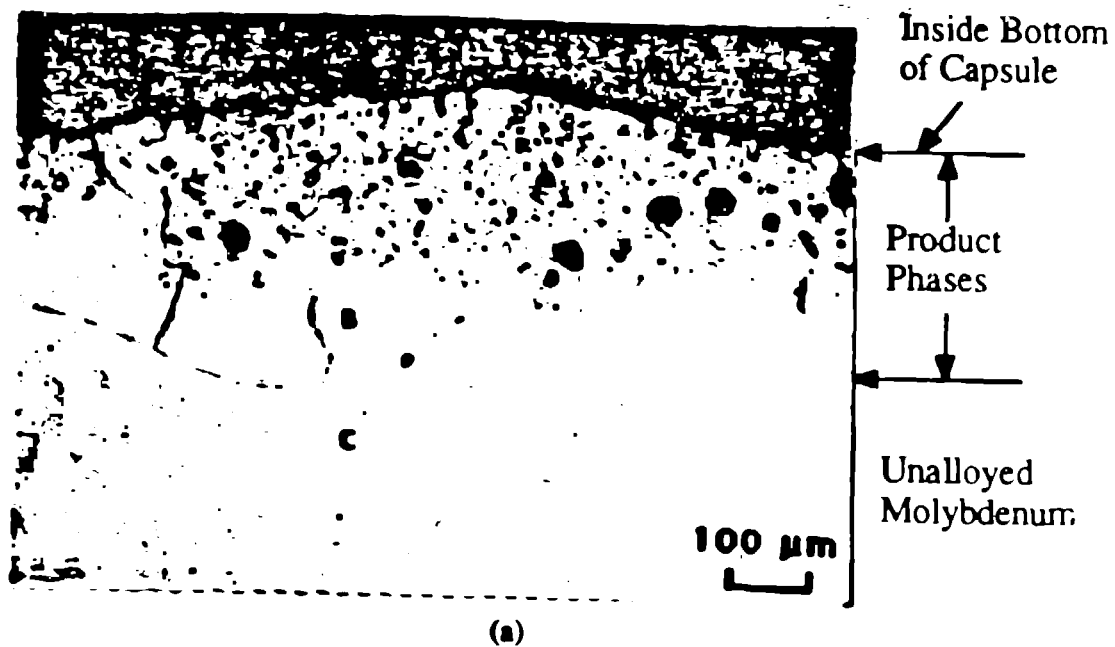

Fig. 4. Optical image of the cross-section of the bottom of the capsule that contained UO_2 and lithium for 10 h at 1450 K (a) and a higher magnification secondary electon image (b) of the boxed area in (a).

As seen in Fig. 4, the microstructure near the interior surface of the capsules indicates that the material in this region was a mixture of solid and liquid material during the heat treatment. The rounded structures appear to have been molten at the end of the experiment. The electron microprobe examinations indicated that these rounded structures marked A in Fig. 4(b) contained

only uranium. However, there was a small deficit in the total amount of material indicated by the electron microprobe in this phase suggesting that lithium might also be present. The voids seen in these uranium globules might also contribute to the lack of complete material accountability in these structures. The matrix material, marked B in Fig. 4(b), was measured and found to contain 34 at.% Mo and 66 at.% U.

3. 1525 K Capsule Data

The microstructural features typical of the cross-section of the bottom of the capsules heated 10 h at 1525 K can be seen in the photomicrographs in Fig. 5. In some respects, this microstructure is very similar to that in the sample that had been heated at 1450 K except that the two-phase regions seen in the photomicrograph in Fig. 5(a) are no longer a continuous band across the field of view. As with the samples from the other two heat treatments, at least three phases besides pure molybdenum are seen in the microstructures in Fig. 5(a). The rounded features seen in photomicrographs in Fig. 5 appear to have been molten at the end of the anneal period, while the remainder of the structure seems to have been solid at that point in time. Voids appear in the two-phase region as previously seen in the 1450 K sample.

A careful examination of the microstructural features between the positions marked A and C in Fig. 5(a) reveals a series of cracks that tend to run through a zone bounded on one side by the C region and on the other by the A region. The interface region marked by the end of the cracks coincides both with the location of the transition between a highly air-reactive alloy and a relatively air-stable alloy.   The electron microprobe data indicated that the uranium content fell to 63.6 at.% at the A-C interface. The phase marked A in Fig. 5(` ` appears to be the same as that marked A in Fig. 5(a).

The angular precipitate marked B in Fig. 5(b) was analyzed with the electron microprobe to contain only uranium but with somewhat less than 100% recovery of the material present. In a second analysis, significant quantities of carbon were found in these microstructural features with the electron microprobe in addition to uranium. However, the carbon concentration was well below that required to indicate the presence of stoichiometric UC. Only 93-94% of the mass was accounted for in this analysis. Ion microprobe analysis of a nitrogen ion-milled area similar to that seen in Fig. 5(b) indicated lithium was also present in the angular shaped particles but not in the rounded ones.

Two electron microprobe scans were made from the bottom surface of the capsule inward across the apparent single-phase area marked A in Fig. 5(a) prior to the removal of the oxide coating. The bulk composition of the underlying alloy was obscured from the electron microprobe by the oxide layer until the molybdenum content reached 18 at.%. The transformed concentration-position data obtained from an electron microprobe step-scan starting from the point where the oxide layer was not detected is plotted in Fig. 6. The uranium content ranged from 79 to 63.6 at.% in this scan inward across the A-region. The logarithm of the uranium content versus

the square of the diffusion distance for this composition region is seen to be well represented by a straight line. An interdiffusion coefficient of 3.2×10^{-9} cm^2/s is derived from a linear least-squares fit to the data plotted in Fig. 6.

Inside Bottom of Capsule

Product Phases
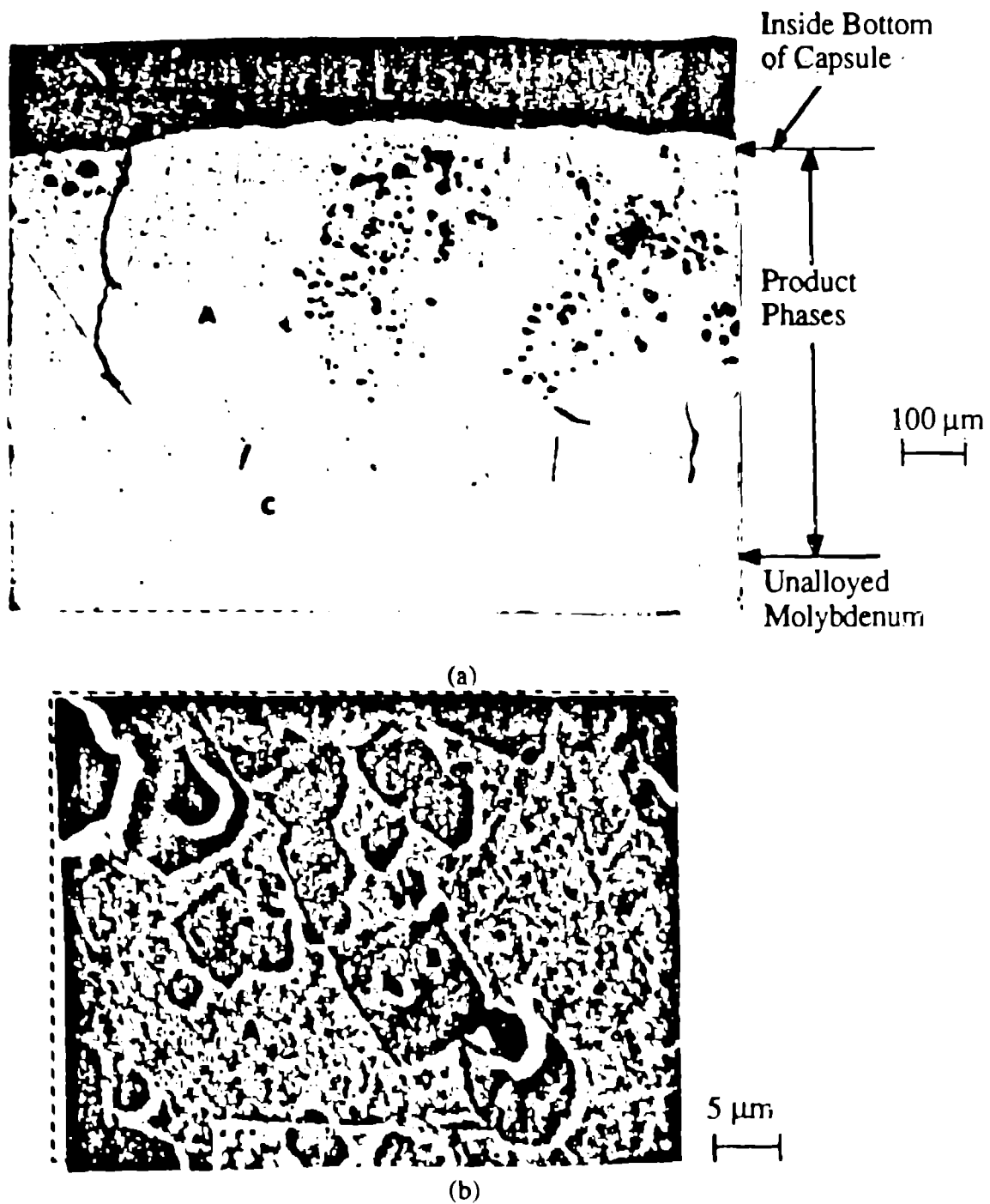
100 μm

Unalloyed Molybdenum

(a)

5 μm

(b)

Fig. 5.   Optical image of the cross-section of the bottom of a molybdenum capsule that contained lithium and UO$_2$ for 10 h at 1525 K(a) and a higher magnification secondary electon image (b) of the boxed region in (a).
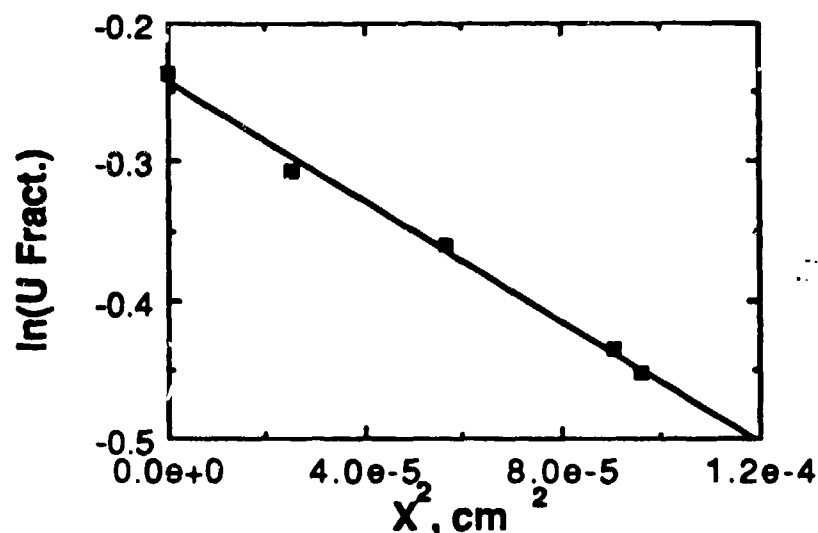
Fig. 6.   Concentration-position over the range 64 to 79 at.% U in the U_2Mo phase (adjacent
           to the molybdenum-rich solid-solution phase) in a capsules heated 10 h at 1525 K.

Two addtional electron microprobe scans were made on this sample after the oxide layer was
removed by mechanical polishing. These data are represented in Fig. 7. The uranium content in
these two scans of this single-phase region ranged from 87.1 at.% at a point 10 μm from the
bottom of th: capsule to 79 at.% at a point 390 μm inward from the bottom. These data where
fitted to two separate straight line segments that intersect at a uranium content of about 84 at.%.
The diffusion coefficient derived from the curve above 84 at.% U was $1.6x10^{-7}$ cm^2/s, while
below 84 at.% U, the diffusion coefficient was calculated to be $8.7x10^{-8}$ cm^2/s. These results
seem to complete a trend toward increasing interdiffusion coefficients with uranium content in this
single-phase region.

Similar to the lower temperature samples, the region designated C in the photomicrograph in
Fig. 5(a) appears to be the molybdenum-rich solid solution phase which were found by the electron
microprobe to contain 1-2 at.% U. The thickness of this phase measured from 50 to 80 μm in both
samples which yields interdiffusion coefficients of 2 to 4 x 10^{-10} cm^2/s, respectively.
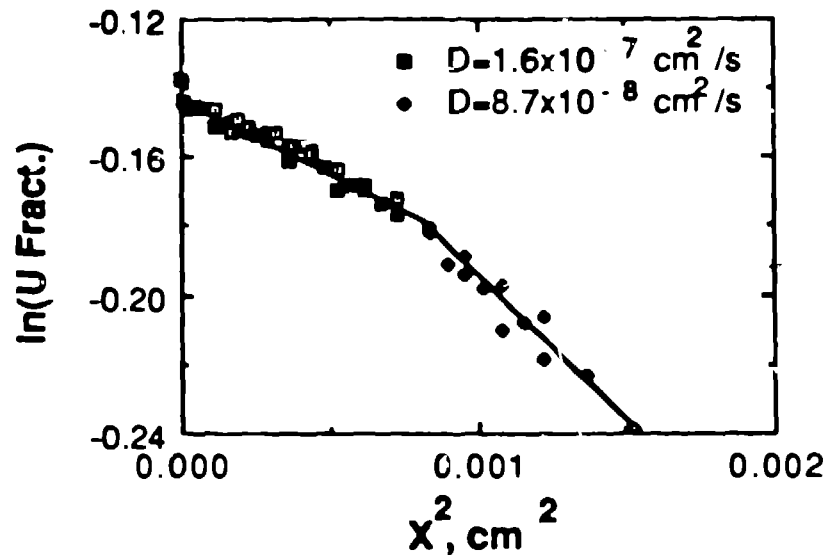
Fig. 7. Concentration-distance data from the U_2Mo phase in a capsule heated 10 h at 1525 K.

III. Discussion

The interdiffusion data obtained in this study were compared with the few values found in the literature. Comparisons with published interdiffusion coefficients of uranium and molybdenum can only be made by extrapolating the published values to the temperatures of this study. Interdiffusion coefficients for high uranium contents extrapolated to 1400 and 1525 K from lower temperature data published by Adda and Philibert [4] are plotted, in Fig. 8, along with values obtained in this study. The comparison, which is only possible at 1525 K, is reasonable. The reduction of diffusivity with temperature in the uranium content range 64 to 79 at.% is surprising, but it might be indicative of another phase distinct from U_2Mo. The diffusivities measured for the low uranium content phase increase with temperature which is the normal pattern.

The interdiffusion coefficients obtained in this study for the low uranium contents can be compared with a value derived from data at 1366 K published by DeCresente, et al [6] for solid-state reactions between molybdenum and UO_2. A value of 1.5×10^{-11} cm^2/s was calculated from these published data which is comparable to the 1400 K value in the present study, 3.6×10^{-11} cm^2/s.

The interdiffusion data presented above indicates that for the temperature range 1400 to 1525 K the U-Mo system includes: (1) a molybdenum-rich solid solution, Mo[U]; (2) an intermediated phase, which appears to be an intermetallic compound, U_2Mo; and (3) liquid uranium. The liquid uranium globules probably contained dissolved molybdenum at some concentration level below the detection limit of the electron microprobe for molybdenum, which is approximately 0.5 at.%, and

thus it appears to be the terminal solution of molybdenum in uranium, U[Mo]. The compositional limits of these phases indicated by the data. except for U[Mo] for which we only have upper bound estimates, are summarized in Table II.
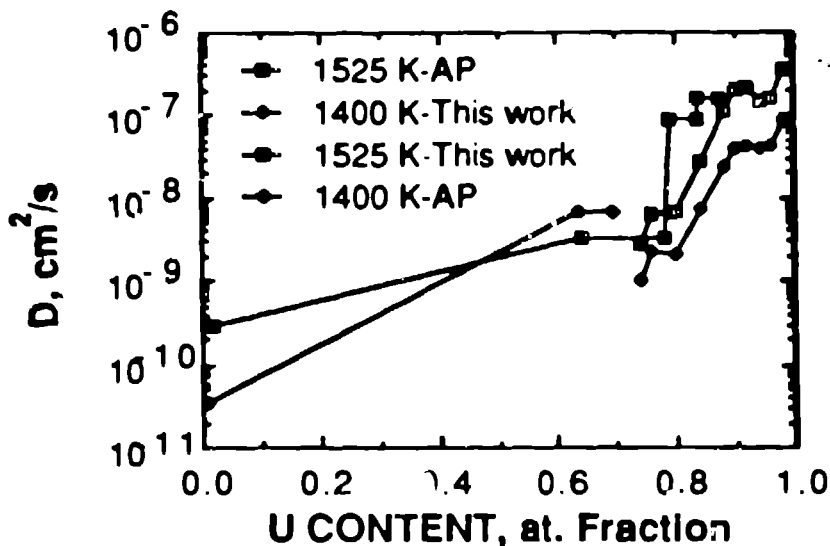

Fig. 8. Comparison of interdiffusion coefficients as a function of uranium concentration in U-Mo derived from this work with those published by Adda and Philibert [4] (AP).

Table II.   U-Mo phase boundary compositions determined from electron microprobe analysis of the metallographic sections of the molybdenum capsules.

Boundary Concentrations (at.% U)

Temperature (K)	Mo[U]	Mo[U]+U_2M ,	U_2Mo+U[Mo]
1400	1.1	63.6	69.2
1450	1-2	62.	70.
1525	1-2	63.6	87.1

The phase boundary data for the molybdenum-rich solid solution, Mo[U], derived from this study for the temperature range 1400 to 1525 K is generally consistent with that found in the Brewer. et. al. [1] diagram. However, the solubility of uranium in molybdenum obtained in this study is slightly lower than indicated in the Brewer. et. al. [1] diagram.

The accepted phase diagram [1] indicates that U_2Mo, which is reported [7] to be tetragonal,

decomposes around 875 K to form γ-U[Mo] which has a body-centered-cubic structure. The data from this study indicates that the U_2Mo phase extends to 1525 K which is close to the reported [1]

peritectic temperature, 1557 K, and the x-ray diffraction data indicate that the U$_2$Mo-phase quenched from 1400 K is close-packed hexagonal. The range of compositional stability of the U$_2$Mo phase appears to increase with temperature by expanding to higher uranium content. The lower uranium content boundary of the U$_2$Mo phase seems to be nearly constant with temperature.

The purity of most of the alloys on which the published U-Mo phase diagram is based is highly suspect, especially in the high uranium content regions where the chemical reactivity of the alloy is quite high. Even the early reviewers [9] of the U-Mo system recognized this fact. Microstructures of many of the alloy samples studied were reported to include oxide or carbide particles, which implies that the solubilities of these two elements was generally exceeded in the samples. With the exception of the angular structures seen at 1525 K, precipitates were not seen in the alloys formed by interdiffusion in this study.

In general, data on the chemical composition of the heat treated samples from the older studies are lacking for the heat-treated condition. These data are especially needed to give credibility to the phase equilibria deduced from observations on samples that were annealed for long times at high temperatures in containers made from materials such as silica that can react chemically with metallic uranium. The purities of the alloy phases formed in the current study were confirmed by the microprobe analyses of the interdiffuison zones.

An effort was made to reconcile the tracer diffusion data from the literature [2], [8] and the interdiffusion data for U-Mo using the phase equilibria inferred from this study and Darken's equation that defines the link between the thermodynamic driving forces and interdiffusion in binary alloys. The equation for calculating Darken's thermodynamic factor from the interdiffusion coefficent, D_{U-Mo}, and tracer diffusion coefficients, D^*, is presented below:

$$\frac{D_{U-Mo}}{D_U^*(1 - N_U) + D_{Mo}^* N_U} = 1 + \frac{d\ln \gamma_U}{d\ln N_U}$$

N_U is the uranium atom fraction appropriate to the D^* for that composition, and γ_U is the activity coefficient for uranium in the same U-Mo alloy. The Darken factor, which is the righthand term above, is related to the free energies of the different species, but the free energy values cannot be derived directly from the Darken factor. Never-the-less, rapid changes in the Darken factor values are usually seen at compositions close to phase boundaries.

Calculations were first performed to compare the D_{U-Mo}'s between Mo[U] and U$_2$Mo with the experimental interdiffusion coefficients determined in this and other studies [6]. The thermodynamic coefficients for Mo[U] were taken from Brewer, et. al. [9], and the impurity diffusion coefficients were taken from Fedorov and Smirnov [8]. The theoretical results are

compared with experimental values in Table III. The agreement between the calculated and observed values is quite reasonable considering the limited data.

Table III. Comparison of calculated and experimental interdiffusion coefficients in the Mo[U] phase.

Temperature (K)	$D_{U.Mo}$ (10^{-11} cm^2/s) Calculated	Experimental	Experimental Data References
1366	4.1	1.5	[6]
1400	6.5	3.6	This work
1450	12	40	This work
1525	30	20	This work

Darken thermodynamic factors were calculated from U-Mo interdiffusion data for the high uranium content region. A representative set of results for molybdenum contents ranging from 5 to 30 at.% are plotted in Fig. 10. This data set, which is for 1273 K, is based on tracer diffusion data from Fedorov and Smimov [2] and interdiffusion data from Adda and Philibert [4]. It was necessary to extrapolate the interdiffusion data for the value at 30 at.% Mo from data at 25 at.% Mo. The value of the Darken factor calculated from this extrapolated interdiffusion data is very
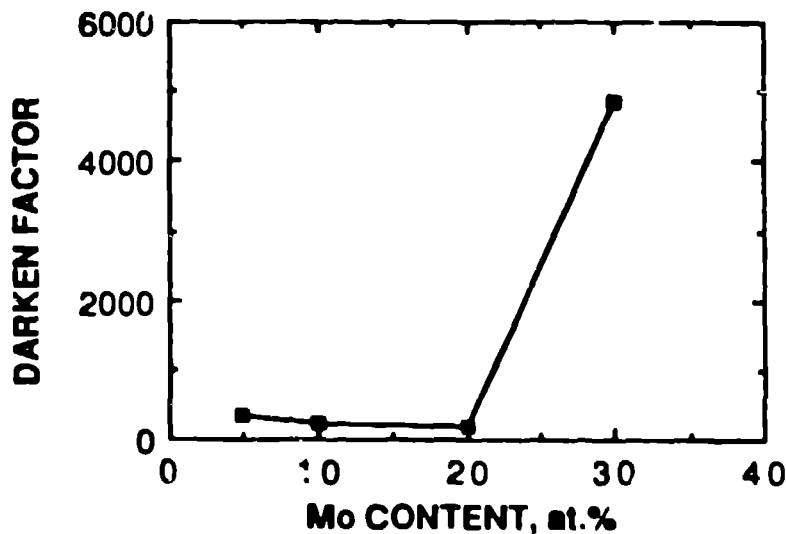

Fig. 10. Darken thermodynamic factor calculated from U-Mo diffusion data ([2] and [4]) at 1273 K.

close to a value calculated at 1400 K from interdiffusion data obtained in this study and a temperature extrapolation of Fedorov and Smimov's tracer diffusion data. It is significant that the calculated thermodynamic coefficient values show a very rapid change near the U$_2$Mo+U[Mo]-U$_2$Mo phase boundary composition indicated by this study. The limited thermodynamic data on

the U-Mo alloy system [5] do not disagree with the extension of the U_2Mo phase to high temperatures nor do they conclusively support it.

IV. CONCLUSIONS

Even though the data presented here on the interdiffusion of uranium and molybdenum are incomplete, they point to a need for a significant correction to the high temperature region of the presently accepted U-Mo equilibrium. These data show that the U_2Mo phase extends to temperatures much higher than stated in previously published literature. Extension of the intermediate phase U_2Mo to higher temperatures allows the interdiffusion data for uranium and molybdenum to now be reconciled with the U-Mo phase equilibria on the the basis of thermodynamic considerations. An analysis of the existing U-Mo interdiffusion data reveals that the activity coefficients are changing rapidly near the experimentally indicated $U_2Mo+U[Mo]-U_2Mo$ phase boundary as would be expected.

Because these conclusions are based on a limited amount of data, a final definition of the high temperature regions of the equilibrium U-Mo phase diagram will require further study. It is clear that isothermal interdiffusion of the elements is a very useful technique for studying the high temperature regime.

References:

[1]   L. Brewer, R. H. Lamoreaux, R. Ferro, R. Marazza, and K. Girgis: *Molybdenum: Physico-Chemical Properties of Its Compounds and Alloys*, Atomic Energy Review, Special Issue No. 7, L. Brewer, Ed. (IAEA, Vienna, 1980) pp 336-338.

[2]   G. B. Fedorov and E. A. Smirnov: *Diffusion In Reactor Materials* (Trans Tech Publications, Switzerland, 1984) Translation of *Diffusiya. v Reactornykh Materialakh*, Atomizdat Publishers, Moscow ,1978) pp 97-98.

[3]   P. G. Shewmon, *Diffusion in Solids* (McGraw-Hill Co., NY, 1963) p. 126.

[4]   Y. Adda and J. Philibert, *C. R. Acad. Sci.*, 246, 1 (1958) pp. 113-116.

[5]   Yu. V. Vamyerskii, A. L. Udovskii, and O. S. Ivanov, *Thermodynamics of Nuclear Materials*, Vol II. (IAEA, Vienna, 1975) pp. 321-336.

[6]   M. A. DeCrescente, M. S. Freed, and S. D. Caplow, Report No. PWAC-488, Pratt & Whitney Aircraft Company, October 1965.

[7]   A. E. Dwight, *J. Nucl. Mat.*, 2, 1 (1960) p. 81-87.

[8]   G. B. Fedorov and E. A. Smirnov, *Diffusion in Reactor Materials,*"((Trans Tech Publications, Switzerland, 1984 (Translation of *Diffusiya. v Reactornykh Materialakh,* Atomizdat Publishers, Moscow, 1978)) p. 78.

[9]   L. Brewer, R. H. Lamoreaux, R. Ferro, R. Marazza, and K. Girgis, *Molybdenum: Physico-Chemical Properties of Its Compounds and Alloys* (Atomic Energy Review, Special Issue No. 7, L. Brewer, Ed., IAEA, Vienna, 1980) p. 172.